Online Yarn Breakage Detection: A Reflection-Based Anomaly Detection Method

Ning Yan (闫宁), Linlin Zhu (朱琳琳), Hongmai Yang (杨宏脉), Nana Li (李娜娜), and Xiaodong Zhang (张效栋)

***Abstract*— This article discusses an optical reflection-based method for equipment anomaly detection that enhances weak signals and has high sensitivity to abnormalities. Automatic warp knitting machine yarn breakage detection, which has become an acknowledged difficulty in the textile field, is achieved. To the best of our knowledge, this is the first time that visual inspection has been applied to yarn breakage detection in weaving. Furthermore, based on the periodicity of the yarn distribution and the periodic motion law of the machine, the combined wavelet and Seasonal and Trend decomposition using locally weighted regression (LOESS) (STL) decomposition method is proposed for yarn breakage detection. Finally, the efficiency and accuracy of the proposed method are verified experimentally. Our research is a successful application of reflection characteristics to the anomaly detection of non-Lambertian objects, which has implications for the high-precision anomaly detection of precision equipment.**

***Index Terms*— Anomaly detection, reflection method, warp knitting, yarn breakage detection.**

I. Introduction

IN THE macroscopic field, ray propagation strictly conforms to the laws of geometrical optics; therefore, taking light as the standard has always been regarded as a high-precision measurement method. For example, methods, such as theodolite [1], linear structured light [2], and fringe projection measurement [3], achieve high-precision measurements based on the concept that light travels in straight lines. Optical reflection can magnify small features, and it has been verified that measurement based on reflection can achieve higher accuracy [4], [5]. In addition, based on the sensitivity to the pose, the optical reflection-based optical lever is widely used in precision equipment such as atomic force microscopy [6] and gravitational wave detection equipment [7]. Optical detection is an important branch of optical applications, and the use of optical reflection also provides an idea for high-precision detection [8]; however, the traditional structures to be tested do not have mirror features, which make them difficult to detect using the traditional reflection method [9], [10]. In fact, most of the structures are non-Lambert objects, which have certain reflective properties; however, this kind of reflection is very different from the reflection of mirrors and is difficult to use. In this article, we conducted our research on automatic warp knitting machine yarn breakage detection; our motivation is to solve the acknowledged problem of automatic warp knitting machine yarn breakage detection and propose an optical-reflection-based method for high-precision non-Lambert object anomaly detection.

Warp knitted fabric is an important source of high-end clothing, home textile fabrics, and basic materials of high technology [11]–[13]. However, yarn breakage is inevitable in the weaving process and is considered to be the cause of nearly 70% of fabric defects according to research. When yarn breakage occurs, it is necessary to stop the machine immediately for yarn repair to avoid quality degradation of the final finished fabric. However, the detection of yarn breakage has always been a difficult problem in the warp knitting industry. First, yarns are thin and dense. One example is the RD7-2/12 warp knitting machine produced by Karl Mayer Company (see Fig. 1). In the machine that is approximately 4-m long, the distance between adjacent yarns is only 1.1545 mm [see Fig. 1(b)]. Therefore, physical sensors for yarn detection cannot be used in warp knitting machines considering the costs and equipment structure [14]–[17]. Furthermore, yarns can be as thin as tens of microns, creating difficulties to visual inspection. For a typical case, the yarn diameter is 100 μm, and the camera lateral resolution is 1000. If a single column of pixels corresponds to a single yarn, a single camera can only cover 0.1 m (100 μm $\times$ 1000), meaning that nearly 40 cameras are required to cover the whole area, which is obviously unrealistic. Second, the yarns of different guide bars are always interweaved together. When the yarn of a certain layer breaks, the image of all other layers of yarns is an interference signal at this time. Due to the interference of each yarn, which introduces considerable noise, the information of yarn breakage is very weak [see Fig. 1(c)].

As a high-precision detection method, optical detection is a mainstream research direction of yarn breakage detection.

Manuscript received January 18, 2021; revised March 20, 2021; accepted March 23, 2021. Date of publication April 5, 2021; date of current version April 27, 2021. This work was supported in part by the National Key Research and Development Program of China under Grant 2017YFA0701200, in part by the Science Challenge Program under Grant TZ2018006-0203-01, and in part by the Natural Science Foundation of Tianjin under Grant 18JCZDJC37000. The Associate Editor coordinating the review process was Dr. Jing Lei. *(Corresponding author: Xiaodong Zhang.)*

Ning Yan, Linlin Zhu, Hongmai Yang, and Xiaodong Zhang are with the State Key Laboratory of Precision Measuring Technology and Instruments, Center of Micro/Nano Manufacturing Technology, Tianjin University, Tianjin 300072, China (e-mail: zhangxd@tju.edu.cn).

Nana Li is with the School of Textile Science and Engineering, Tiangong University, Tianjin 300387, China (e-mail: linana_tj@126.com).

Digital Object Identifier 10.1109/TIM.2021.3071227

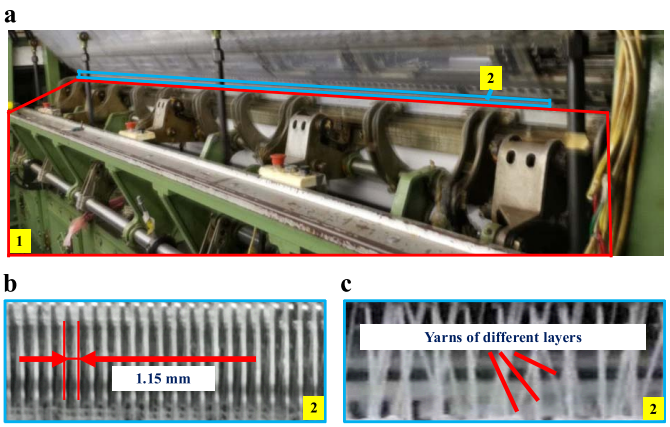

Fig. 1. RD7-2/12 double needle bar raschel machine produced by Karl Mayer. (a) is an external view of the warp knitting machine, and the length of which is approximately 4 m. Area 1 shows that the fabric is obscured by the mechanical structure, and area 2 is the weaving area. At different weaving times, (b) and (c) can be obtained separately by enlarging area 2 of (a). (b) shows the needles in the first layer, and the density of the needles determines the maximum density of the yarns. (c) shows the yarns, where it can be seen that multiple layers are interweaved.

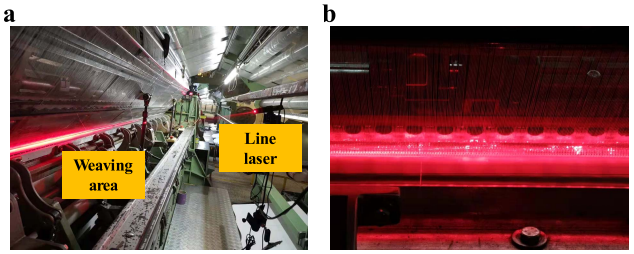

Fig. 2. Yarns highlighted with a line laser, in which (a) is the detection system, and (b) is the captured result. This method is inspired by Musa [18] and [19].

Musa [18] and [19] used a line laser to project characteristic points on yarns and then used a camera to capture the highlighted yarns to detect yarn breakages. Although this method can be used to enhance yarn characteristics, it cannot solve the problem of multiple yarns interweaved. As shown in Fig. 2, we have tested this yarn enhancement method in a warp knitting machine. All yarns are highlighted at the same time, and the signal and noise are enhanced synchronously, causing yarn breakage detection to be difficult. Therefore, most of the existing yarn breakage detection methods aim at the features caused by broken yarn to achieve indirect detection. A relatively mature yarn breakage automatic detection method is based on fabric defect detection because the broken yarn will produce marks on the fabric [20]–[24]. However, this method has large limitations because it is effective only when the fabric surface is completely exposed. For the double needle bar raschel machine [see Fig. 1(a)], due to the complexity of the mechanical structure, the fabric is obscured for up to 1 m after weaving. If yarn breakage is not detected in a timely manner, many defective fabrics will be produced, and the broken yarn may cause other yarns to break, which will seriously affect the normal operations of a machine. The German enterprise Protechna developed a product in which a set of lasers and photoelectric sensors are installed in the neighborhood of each layer of yarns. When a yarn breaks, it will float out under the action of the blower and obscure the light of the laser. Then, the photoelectric sensor detects the change in light and judges the existence of yarn breakage. However, this method is essentially an indirect method. Because sometimes yarn will be entangled after the yarn breaks and will not float, the opportunity for inspection may be missed, and the timeliness of this method also needs to be improved.

In our opinion, the most direct method is the most effective, so we focus on studying how to detect yarn breakage by directly capturing the yarns in the weaving area where yarn breakage occurs. The key to solving this problem is to extract the weak broken yarn signal from the strong noise. Our method in this article is based on the non-Lambert body reflection characteristics. When the incident light hits the yarn, a considerable amount of the reflected light will travel along the reflection direction. By arranging the camera in the outgoing direction of the light, a large amount of information will be captured by the camera so that the camera can obtain super-resolution information, allowing the camera to shoot with a large field of view. Furthermore, based on the characteristic that the law of reflection is very sensitive to the posture of yarns, the yarns of different guide bars can be distinguished and detected separately so as to avoid the interference of yarns of different guide bars.

Through the above hardware optimization methods, the signal quality is greatly improved. However, regarding the algorithm, how to achieve stable and reliable detection is still a great challenge. Taking a 4-m-long machine as an example, if the yarn density is 50%, the machine has five layers, and the distance between adjacent yarns is 1.1545 mm. It can be calculated that the machine has $4000/1.1545/2 \times 5 = 8662$ yarns. If five images are taken per second, 0.7 billion yarns will be captured every day. If the number of false positives should be controlled within five times, it can be calculated that the false positive rate (FPR) should be less than 7e−07%, and the high stability requirement will bring great challenges to the algorithm. In order to meet the high stability requirements for the algorithm, considering the periodic motion of the warp knitting machine in the weaving process, time domain anomaly detection and spatial domain anomaly detection are combined to achieve high robustness.

Existing methods for anomaly detection in the spatial domain can be divided into two categories. The first is based on deep learning. In recent years, with excellent fault tolerance and adaptability to new data, deep learning has shown excellent performance on many complex nonlinear processes, which are very difficult to solve using traditional methods [25]. In the field of textile defect detection, methods related to deep learning can be divided into unsupervised learning and supervised learning; method based on unsupervised learning does not need to mark defects in advance, which is much more convenient than supervised learning in use, and can also solve the problem of defect data scarcity. Hu *et al.* [26] present an unsupervised method for automatically detecting defects in fabrics based on a deep convolutional generative adversarial network (DCGAN). By subtracting the original image from

the image generated by DCGAN, defects are highlighted while removing the texture. However, although unsupervised learning is an important direction of future development, its accuracy and efficiency are still inferior to supervised learning at present [27], and method based on unsupervised method is difficult to detect weak defects. The methods based on supervised learning can be mainly divided into three categories; the first is based on classification network [28], [29], and this method divides the image into defect image and defect-free image based on classification network; however, when the proportion of defects in the image is very small, the detection accuracy will be significantly reduced. The second method is based on object detection; faster R-CNN [30] and Yolo [31], [32] are two of the typical model and have been used in fabric defect detection and achieved good detection accuracy. The third method is based on semantic segmentation [33], and this method can realize the pixel level segmentation of defects; however, it is generally inefficient and the process of data set annotation is very complicated. In all, at present, object detection is the most common method in defect detection in textile field, and unsupervised learning is an important direction of future development. However, although methods based on deep learning are potential, when a process is easily defined by a comprehensible mathematical model, traditional computer vision techniques are always able to solve the problem much more efficiently in fewer lines of code than deep learning [34]. Due to the strict periodic distribution of yarns and the decreased reflection effect caused by yarn breakage, the yarn breakage detection problem is not difficult to characterize by a simple mathematical formula. In addition, the generalization ability of deep learning is restricted by the data set, which will also restrict the universality of the system. Therefore, in our opinion, traditional computer vision techniques may be better for yarn breakage detection than deep learning. Therefore, we choose to use traditional algorithm to ensure the stability and traceability of the algorithm. Deep learning, as a very popular method at present, is used for algorithm comparison in this article.

The yarn breakage detection problem can be abstracted as the detection of anomalies in periodic features. Xie [35] discusses texture feature extraction and analysis in four categories. The first category is macrostatistics approaches, such as histogram properties [36], co-occurrence matrices [37], autocorrelation [38], and local binary patterns [39]. The first three methods mainly focus on macro characteristics; therefore, their sensitivity to yarn breakage defect is poor. Local binary patterns are relatively sensitive to small defects; however, they are easily disturbed by texture information. The second category is structural approaches, which detect defects by modeling texture features, which is relatively complex and inflexible [40]. The third category is called model-based approaches, which represent a broad concept and mainly refer to some texture analysis models proposed by scholars, such as fractal models, autoregressive models, and so on. These models can adapt to some complex situations, but the algorithm complexity is always high [41]. The fourth category is filter-based approaches, which highlight defects by removing the interference of texture structure by filtering. Among the filter-based approaches, the wavelet, a time–frequency joint analysis method, is a typical representative method that can locate defects while removing periodic noise [42]. Wavelets are used for anomaly detection in the spatial domain in this article. The key for anomaly detection in the time domain is similar to that in the spatial domain, and it is very important to remove the periodic signal caused by the periodic movement of the machine. The difference is that compared with the signal period in the spatial domain, the signal period in the time domain is strictly fixed; in the time domain, the abnormal signal is at the end of the whole signal. Therefore, for signals in the time domain, signal prediction methods based on statistics are more suitable. For signal forecasting, the classical statistical methods are based on the moving average method, which is easily disturbed by noise [43]. Methods developed on the basis of classical methods, such as X11, Signal extraction in ARIMA time series (SEATS) [44], and Seasonal and Trend decomposition using locally weighted regression (LOESS) (STL) [45], can achieve more robust results. Among these methods, STL is a time series decomposition method that can satisfy different periods, and this method is used for time domain anomaly detection in this article. According to the characteristics of yarn breakage, we also simplified the STL algorithm to improve the detection speed.

Finally, a detection system is built based on the reflection-based shooting method, and the algorithm combines time domain and spatial domain detection. It has been verified by several sets of experiments that the detection system can achieve long-term and stable yarn breakage detection for a warp knitting machine.

Our specific contributions are as follows: 1) the warp knitting machine yarn breakage detection problem is solved, which is a recognized problem in the field of textiles; 2) through the time domain and spatial domain composite method, the robustness of the algorithm is greatly improved; in addition, the STL algorithm is simplified according to the specific characteristics of yarn breakage detection; and 3) the anomaly detection method based on reflection can assist the anomaly detection of other precision equipment that has a non-Lambert surface and periodic motion law, such as defect detection of ceramic tile, glass plate and plastic board, abnormal detection of blade rotation, radial runout detection of shaft, and so on

II. Reflection-Based Weaving Area Yarn Breakage Detection

In this article, the reflection method for weak signal enhancement is used for yarn breakage detection, as shown in Fig. 3. First, because yarns are thin and dense, it is impossible to shoot each yarn clearly; therefore, yarns should be shoot in a fuzzy state, meaning that the yarn breakage will be reflected through the change of local gray level of the image because we cannot distinguish each yarn. Second, because different layers of yarns interweave, the signals of different layers of yarns will interfere with each other; it is a big challenge to avoid mutual interference; we introduced the reflection method, based on the fact that only the yarn

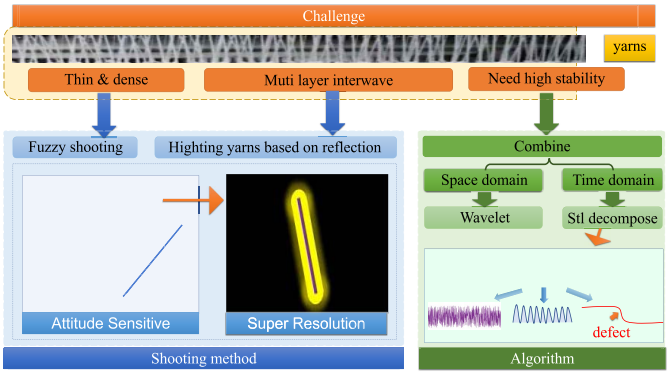

Fig. 3. Sketch map introducing the challenges of yarn breakage detection and the technological process of our method to overcome the challenges.

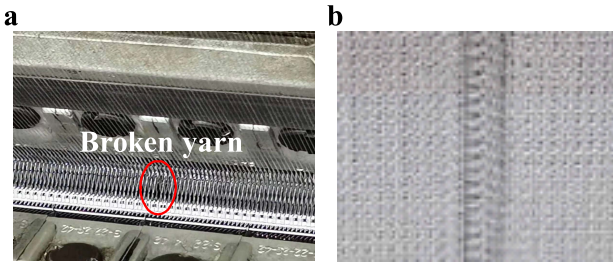

Fig. 4. Yarn breakage capturing result: (a) is an image captured at a short distance where we can see that the broken yarns are difficult to distinguish; and (b) shows the influence of yarn breakage on fabric, where we can see that the feature is very clear.

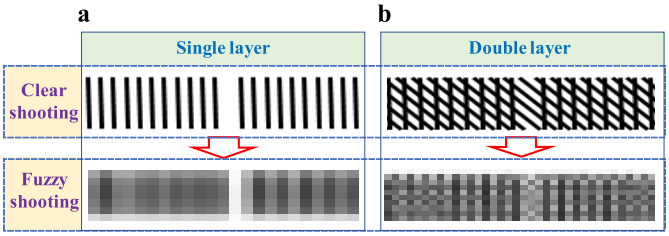

Fig. 5. Schematic of long-distance capturing for (a) a single layer of yarns and (b) double layers of yarns. After a comparison of the upper and lower images, the conclusion can be drawn that blurred shooting may be better for defect extraction.

with a certain angle can be highlighted because of the law of reflection and the fact that inclination angles of different layers of yarns are different; different layers of yarns are highlighted layer by layer, which makes it possible to detect different layers of yarns separately to avoid interference between multiple layers of yarns. At the same time, because a lot of light will be captured by the camera when the law of reflection is satisfied, the camera will get a lot of information of yarns, so as to achieve super resolution. Another big challenge is to meet the needs of high stability. We solved this problem by combining the time domain algorithm and space domain algorithm because the final result is obtained by combining the two methods, and the stability is greatly improved. In the space domain, yarns are distributed periodically; therefore, wavelet is used to extract the periodic signal of yarns and locate the defect. In the time domain, in the weaving process, the light signal of the same pixel has strict periodicity corresponding to the periodicity of the machine. When yarn breaks, the periodicity of the signal is destroyed, and the light intensity decreases. Therefore, we propose a method based on STL decomposition to achieve yarn breakage detection by analyzing whether there is a downtrend in the signal in the time domain.

A. Macro Detection Via Long-Distance Capturing

Yarns are very thin and dense, although they can be clearly captured by pulling the camera closer, as shown in Fig. 4(a). The detection costs will increase significantly because the small field of the camera limits the reduction in the number of cameras, and it is also difficult to obtain yarn breakage information because of the interweaving of multilayer yarns. Therefore, many scholars tend to detect yarn breakage through fabric photography, as shown in Fig. 4(b). In the final finished fabric, although it is difficult to see all yarns, yarn breakage information can still be obtained. Therefore, it is considered that yarn breakage information can be obtained even if the yarn breakages are not photographed clearly. Based on this idea, this article obtains macro information on yarns through long-distance capturing, and yarn breakage is detected via means similar to fabric defect detection.

Fig. 5 shows the schematic of long-distance capturing. Fig. 5(a) is the schematic of single-layer yarns in the case of long-distance capturing, and Fig. 5(b) shows the schematic of double-layer yarns in the case of long-distance capturing. The figure shows that the yarn breakage information is manifested by the absence of yarn at the corresponding position in the case of close capturing. However, in the case of long-distance capturing, yarn breakage information is represented by an abnormal gray level. The most intuitive information of the image is the gray level. Therefore, it is easier to detect defects through image processing by using long-distance photography.

B. Improve the Signal-To-Noise Ratio (SNR) Based on Reflection

By comparing Fig. 5(a) with Fig. 5(b), it can be found that the yarn breakage information obviously weakens as the number of yarn layers increases; however, in the actual weaving process, there may be many layers of yarns in different guide bars. The yarn breakage signal of a certain layer is submerged in the interference signal generated by the multilayer yarns, which makes the signal difficult to extract. Therefore, it is necessary to improve the SNR for yarn breakage detection by considering the distribution and movement of different layers of yarns. In this article, each layer of yarns is individually highlighted based on the reflection characteristics of the yarns. The specific principle is shown in Fig. 6. P is the location of the light source, C is the location of the camera, M is the weaving area, l_3 is the yarns to detect, α is the angle between the line PM and the horizontal direction, β is the angle between the line CM and the horizontal direction, and γ is the angle between the normal direction of yarns and the horizontal direction. Since the textile area is very small, it can be regarded that P, C, and M are three fixed points, which

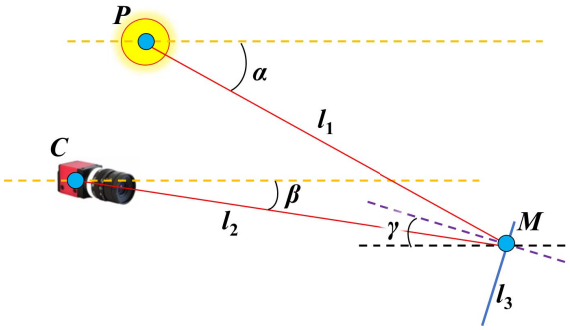

Fig. 6. Sketch map of yarn highlighted based on the law of reflection, where the light produced by light source P is reflected by yarn l3 and shot by camera C.

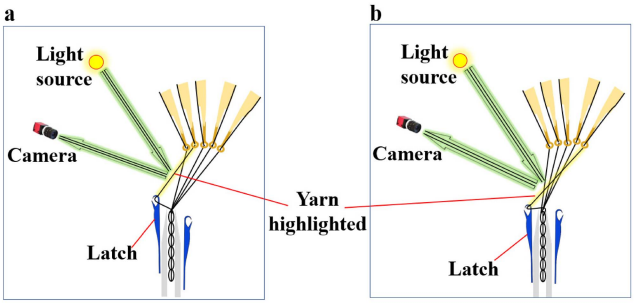

Fig. 7. Sketch map of yarn highlighted by layer. Only the yarn whose angle meets the law of reflection can be highlighted. For example, the No. 2 yarns are highlighted in (a) and the No. 5 yarns are highlighted in (b).

means that α and β are fixed. When the law of reflection is satisfied,

$$\gamma - \beta = \frac{1}{2}(\alpha - \beta) \tag{1}$$

is satisfied, and the corresponding layer of yarns is highlighted.

Because yarns are highlighted based on the law of reflection, a large amount of light is reflected into the camera, and the yarn information is easily captured by the camera. In addition, it can be seen that yarns can only be highlighted when formula (1) is satisfied, meaning that only one layer of yarns can be highlighted at one time so that interference between different layers of yarns can be avoided. During the weaving process, yarns constantly swing back and forth with the movement of the machine, and each layer of yarns can be highlighted separately. As shown in Fig. 7, when the angle of a certain layer of yarns just meets the law of reflection, the layer of yarns is highlighted, and the defects can be identified easily, as shown in Fig. 8.

In the actual weaving process, the amplitude of yarn swinging is often limited. In order to achieve clear capture of all layers of yarns, the adjustable position of cameras and light sources is limited. In addition, it is better to choose the moment when the layer of yarns is not covered by too many other layers of yarns, as shown in Fig. 7, which further limits the position of cameras and light sources. Therefore, it is necessary to comprehensively consider the motion law of the machine tool and the specific weaving process and

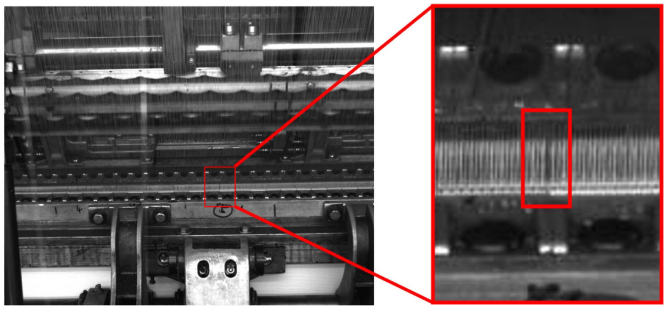

Fig. 8. Image of yarn breakage captured through the method proposed in this article. The left is the whole image captured by the industrial camera. After enlarging the image, we get the image on the right in which the yarn breakage is noticeable.

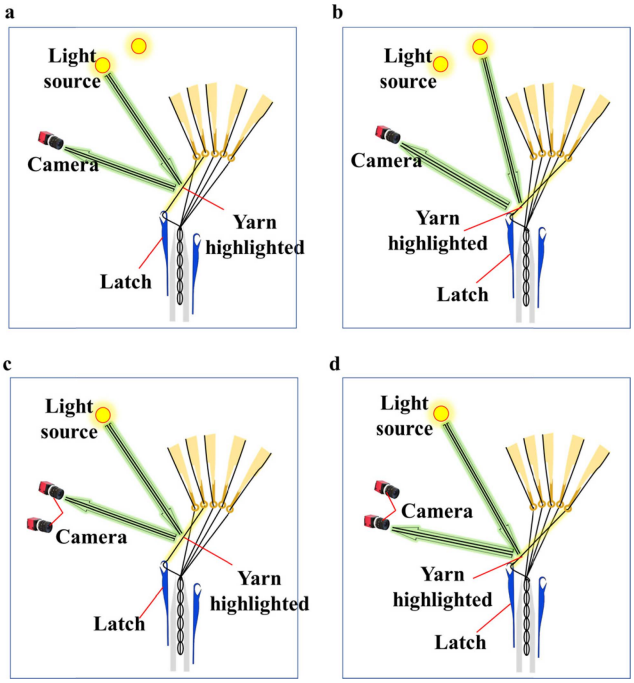

Fig. 9. Sketch maps of yarns highlighted with double light sources and double cameras. (a) and (b) use different light sources to highlight the different layers of yarns. In this method, additional light sources have little impact on hardware costs, but two layers should not be highlighted at the same time in order to avoid mutual interference. (c) and (d) use different cameras to capture the different layers of yarns. In this method, the additional cameras will have a big impact on the hardware costs; however, two layers can be highlighted at the same time because the images of different cameras will not cause interference.

adjust the camera and the light source in the best capturing position using optimizing methods so as to ensure that the yarn breakage of each layer can be photographed clearly. However, because of the restrictions, sometimes there is no solution to the optimization problem. At this time, additional cameras and light sources are needed to add more freedom to the optimization problem. Fig. 9(a) and (b) shows the cases of multiple light sources in which two light sources are set in different positions, providing two incident ray angles α, and different layers of yarns can be highlighted with different light sources. Fig. 9(c) and (d) shows the cases of multiple cameras in which two cameras are set in two positions to shoot different

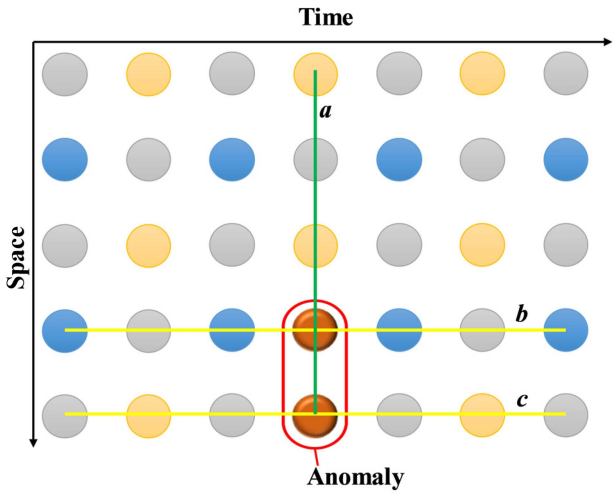

Fig. 10. Yarn breakage in the time domain and spatial domain. The area in red outline represents an anomaly. Yarns are periodic in both domains, and yarn breakage will destroy the periodicity.

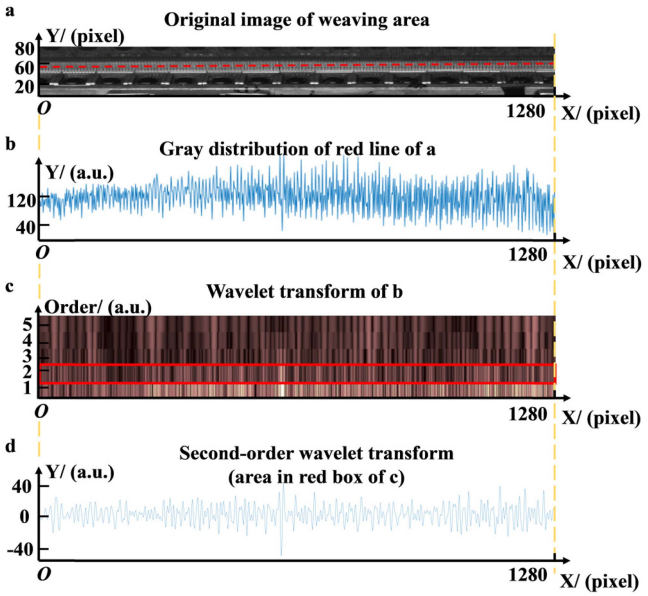

Fig. 11. Wavelet transform used to enhance the feature of the defect. (a) is the original image of the weaving area captured using the method introduced in this article. We obtain the gray value of the red line in (a) and show the result in (b). The defect can be seen, but it is not obvious. (c) shows the results of the wavelet transform in different scales. From the second order, the feature of the defect is very obvious, as shown in (d).

layers of yarns. The figures show that by using the method of multiple light sources or multiple cameras, the optimization problem is easier to solve.

C. Identification of Yarn Breakage Based on Anomaly Detection

Yarn breakage can be extracted from two perspectives. Regarding the spatial distribution, yarn is periodically distributed in the weaving area. When yarn breakage occurs, the original periodicity is broken, as shown in lines a and b in Fig. 10. Regarding the time distribution, the yarn brightness changes periodically during the weaving process, and yarn breakage will also affect the periodicity in the time distribution, as shown in line c in Fig. 10. Detection based on the spatial distribution has strong timeliness. However, the periodicity in the spatial domain is affected by the mapping relations between the camera and weaving area, causing period uncertainty. In addition, a certain extraction method is difficult to apply to different weaving processes. The time domain method detects yarn breakage by analyzing signal anomalies. Because the signal period strictly corresponds to the weaving period of the warp knitting machine, the period of the time domain can be directly obtained through weaving parameters, and the method in the time domain is more stable and pervasive. In this article, a two-step defect extraction algorithm is proposed. First, the periodicity noise is removed via wavelet transformation in the spatial domain. Second, STL decomposition is used to separate the periodic signal and trend signal in the time domain because yarn breakage will decrease the brightness, and the defect can be easily extracted from the trend signal. In addition, to speed up the algorithm, a simplified STL is proposed.

In the time domain, the weaving area of yarns can be divided into three parts. First, the brightness of the weaving area is uneven, which is considered low-frequency noise. Second, some vertical lines can be seen in the weaving area, which can be defined as high-frequency noise. Third, yarn breakage has obvious characteristics in the time domain, which is reflected by local gray abnormalities. Wavelets are a time–frequency method based on which we can obtain the time domain information and frequency domain information of the original signal at the same time. Therefore, in this article, defects are extracted based on wavelets. The Marr wavelet is used because of its similarity to the abnormal area of yarns in an image. The support of the filter is set to $[-7, 7]$. Suppose the number of pixels of an image in the horizontal direction is N. Approximately $15N$ multiplication and addition operations need to be calculated in the wavelet transformation process. The result is shown in Fig. 11. Fig. 11(a) shows the original image to be detected, Fig. 11(b) shows the gray value in the red line position of Fig. 11(a), Fig. 11(c) shows the result of the wavelet transform of Fig. 11(b), and the ordinate represents different scale factors. Fig. 11(d) corresponds to the data in the red box of Fig. 11(c). The defect is highlighted, as shown in Fig. 11(d).

Based on the result of the wavelet transform, a simplified STL decomposition is used to achieve final defect detection [38]. The details are as follows: first, to improve the detection speed, the time of the outer loops is set to 1, and the inner loops of the STL consist of six steps. The first step and the last step are meaningless because the time of the outer loops is set to 1. Second, for each calculation, only a new line of data is added on the basis of the previous data, and most of the data do not need to be recalculated. We use this characteristic to avoid repeated calculations. In the second step, the cycle subseries is smoothed based on LOESS (we set $q = 8$ and $d = 1$). In order to avoid the influence of yarn breakage data on normal

TABLE I
ALGORITHM COMPLEXITY ANALYSIS

Algorithm name	Number of multiplication operations	Number of addition operations
wavelet	15*N	15*N
second step of STL	32*N	32*N
third step of STL		N
fourth step of STL		N

data, only the newly added data are calculated. The main process of this step is local least squares, and approximately $2 \times 2 \times 8 \times N$ multiplication and addition operations need to be calculated. In the third step, moving average filtering is the main process, and we still only calculate the newly added data. Suppose the data period is M. Approximately $(M + M + 3) \times N$ addition operations need to be calculated. In the fourth step and the fifth step, only N addition operations need to be calculated. To provide a clear picture, the number of calculations required for each step is listed in Table I. The complexity of the algorithm is low enough for online detection.

The results of STL are shown in Fig. 12. Fig. 12(a) shows the wavelet-processed signal at different capturing times, and yarn breakage occurs in the middle of detection. The gray values in the same pixel at different times are extracted to obtain the signal in Fig. 12(b), and the results of STL decomposition are shown in Fig. 12(b). The trend signal shows that yarn breakage will cause an obvious decrease in the gray level and is easy to extract by the threshold.

III. RESULTS AND DISCUSSION

A. Construction of the Detection System

The detection system is built, as shown in Fig. 13. The LED fluorescent lamp is selected as the light source, and the image is captured by lens and cameras produced by Hikvision. The specifications and parameters of the detection equipment are shown in Table I. The positions of the cameras and light sources are optimized according to the specific weaving process. The detection system is approximately 1 m away from the weaving area so that the system will not interfere with the textile workers repairing the broken yarn.

B. Feasibility Experiments

To verify the feasibility of the method, six sets of experiments are conducted on three warp knitting machines with three different weaving processes, as shown in Table II. The yarn breakage image obtained in the detection process is shown in Fig. 14, where the images of yarns in the six sets of experiments are very different, and the defects are marked by red boxes. The final results are shown in Figs. 15–20. (a) shows the original signal in the time domain and spatial domain. Only data in the last part of the time domain have yarn breakage. (b) shows the results of the wavelet transform. To a certain extent, the defect is highlighted. (c) shows the results of STL decomposition, where the defect is very obvious. (d) shows the final defect detection results. From the six sets of experiments, the conclusion can be drawn that the proposed method can achieve good detection results for warp knitting machines with different processes.

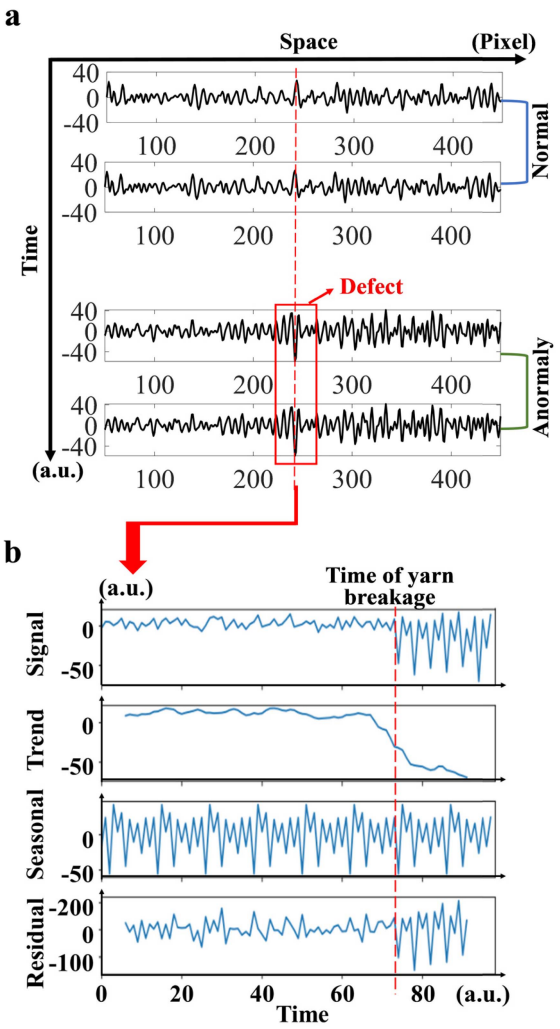

Fig. 12. Defect detection based on STL decomposition: (a) shows the signal extraction process, and (b) shows the defect extraction process by STL decomposition.

TABLE II
HARDWARE DESIGN OF THE DETECTION SYSTEM

	Camera	Lens	Light source
Type	HIKVISION (MV-CE013-50GM)	HIKVISION (MVL-HF1228M-6 MP/ MVL-HF0828M-6 MP)	NVC Lighting
Specification	Resolution (1080*960)	Focal length (12 mm/8 mm)	30 W

C. Comparative Experiments

In order to illustrate the superiority of our algorithm, we conducted two groups of comparative experiments, and the

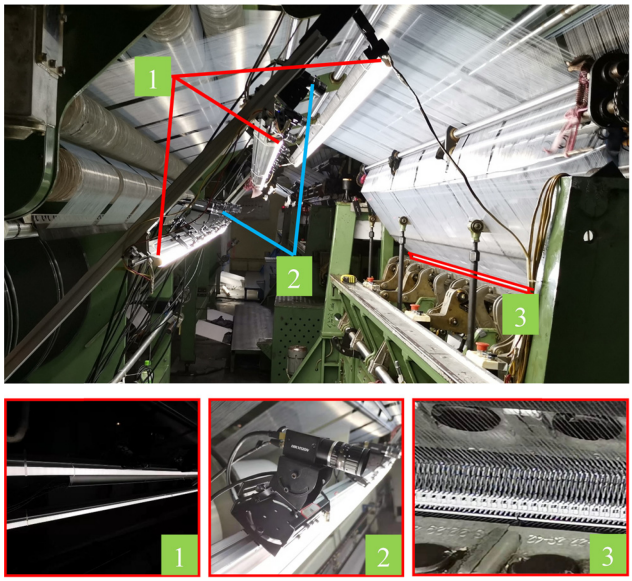

Fig. 13. Yarn breakage detection system including lights and cameras. 1 is the light, which is a common fluorescent lamp. 2 is the industrial camera equipped with a proper lens. To cover the entire field of view, about ten cameras are used. 3 is the detection area, which is also called the weaving area.

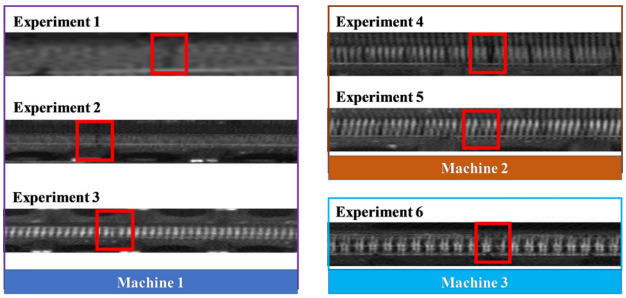

Fig. 14. Yarn breakage images obtained in the detection process of the six sets of experiments, where three different machines are used.

TABLE III
PROCESSING PARAMETERS OF WARP KNITTING MACHINE

Experiment number	Machine number	Guide bar number	Diameter of yarns	Threading process
1	Machine No. 1	No. 1	75 μm	Fully threaded
2	Machine No. 1	No. 2	75 μm	Fully threaded
3	Machine No. 1	No. 4	200 μm	1 in, 1 out
4	Machine No. 2	No. 1	75 μm	Fully threaded
5	Machine No. 2	No. 3	75 μm	5 in, 1 out
6	Machine No. 3	No. 3	200 μm	Fully threaded

data in No.4 experiment of Table III are used for comparison of different algorithms, because the texture is relatively complex in this set of data.

First, in order to verify the stability of our algorithm, we compare our algorithm with the time domain algorithm and

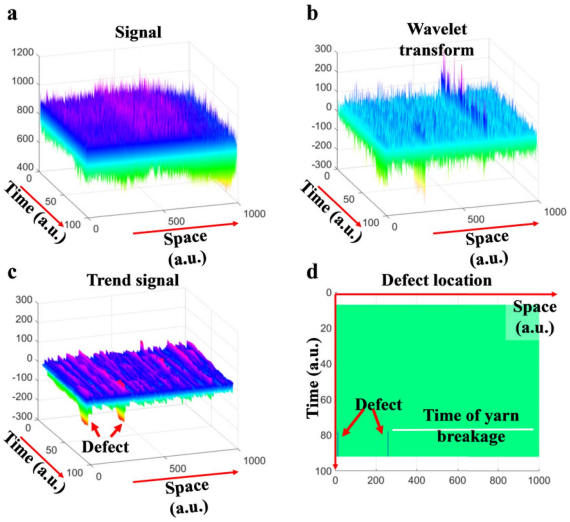

Fig. 15. Detection results of experiment 1. (a) is the original signal in the time and spatial domains. (b) is the results of the wavelet transform. (c) is the results of STL decomposition. (d) is the final detection result.

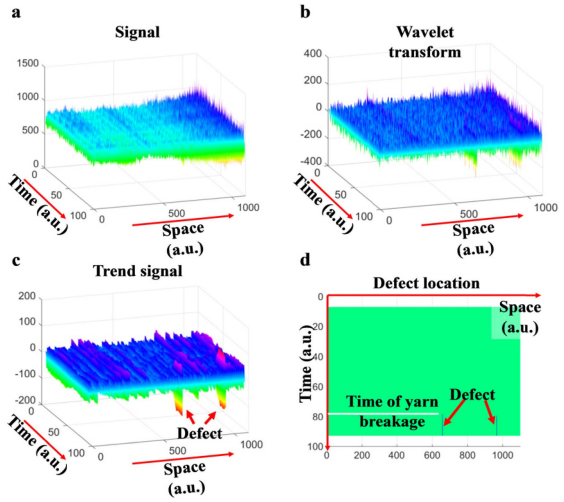

Fig. 16. Detection results of experiment 2. The explanations of (a)–(d) are the same as those in Fig. 15.

spatial domain algorithm separately; two indexes are proposed to evaluate the algorithm; for clarity, we take 1-D signal, as shown in Fig. 21, to illustrate the two indexes, where $f(x)$ is the signal after processed by the corresponding algorithm, the signal of defect starts from $x1$ to $x2$, and the first index is defect to interference rate (DIR), which can be calculated by

$$\mathrm{DIR} = \frac{|K_2|}{|K_1|}. \tag{2}$$

DIR reflects the stability of the algorithm under current data; if DIR is less than 1, the algorithm would be invalid, because the interference is larger than the signal of the defect. The second index is defect to signal rate (DSR), which can be calculated by

$$\mathrm{DSR} = \frac{\int_{x_1}^{x_2} f(x)^2 dx}{\int f(x)^2 dx}. \tag{3}$$

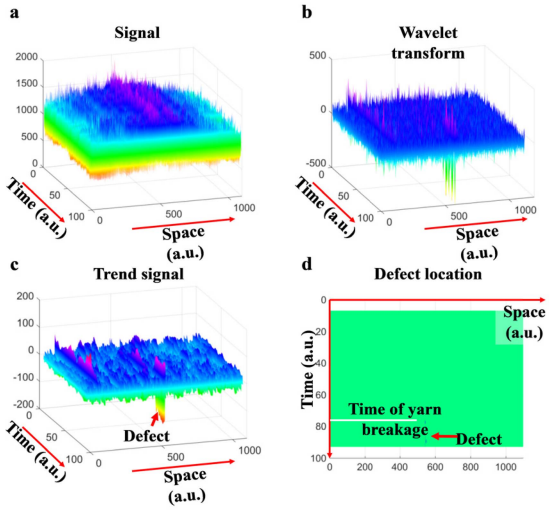

Fig. 17. Detection results of experiment 3. The explanations of (a)–(d) are the same as those in Fig. 15.

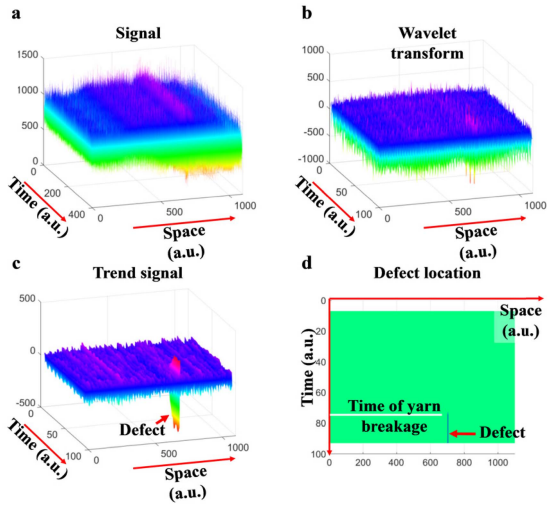

Fig. 18. Detection results of experiment 4. The explanations of (a)–(d) are the same as those in Fig. 15.

DSR reflects the ratio of effective signal and invalid noise, although this parameter cannot directly reflect whether the algorithm is effective, it has more statistical value than DSR because more signals are used. Fig. 22(a) shows the result of the spatial domain algorithm, although it can be seen that the gray level of defect is decreasing; however, there is also a grayscale decline in the normal area because of the textile technology of this machine, causing the method to fail. Fig. 22(b) shows the result of the time domain algorithm, and it can be seen that the noise is not removed effectively. The parametric result is shown in Table IV. It can be seen from the result that DIR and DSR of wavelet and STL decompose are less than 1, meaning that only using wavelet or STL decompose cannot remove noise effectively, and the DIR of the proposed method is 1.6. However, if the noise is not removed by reflection in the process of camera shooting, the noise will be about several times as much, because the signal of different

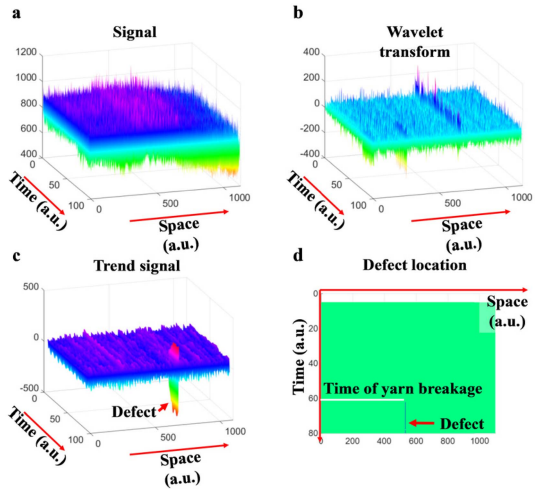

Fig. 19. Detection results of experiment 5. The explanations of (a)–(d) are the same as those in Fig. 15.

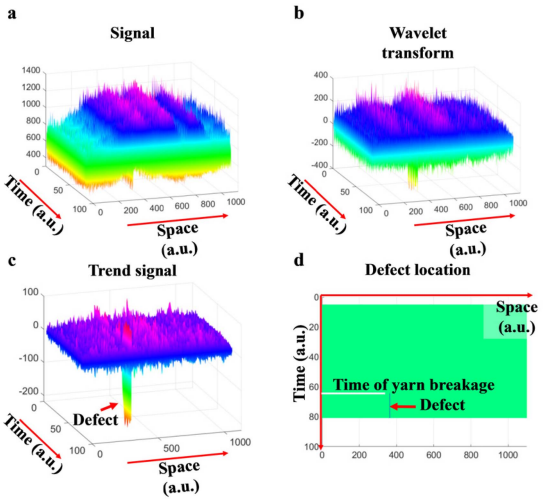

Fig. 20. Detection results of experiment 6. The explanations of (a)–(d) are the same as those in Fig. 15.

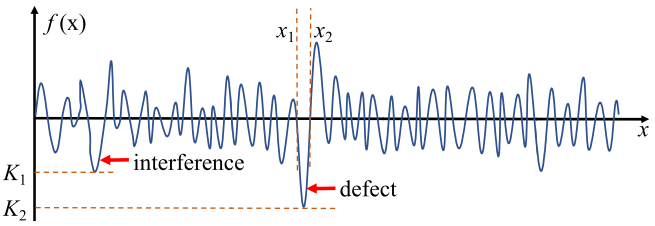

Fig. 21. Simulation of a signal after proposed by algorithm.

layers will superimpose together; at this time, our method will also face the high risk of being invalid.

At the same time, we also use a deep learning model named yolov4 [46] for further comparison, and the model is proposed in 2020, which has more excellent performance than the earlier models. And it has already been used for defect detection [47]. The early version of yolov4 named yolov3 has already been used for fabric defect detection and achieved good results [31], [32].

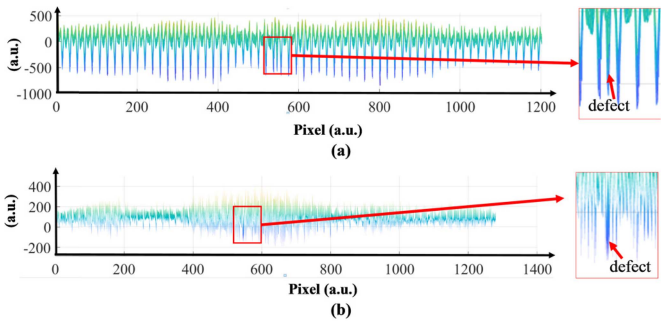

Fig. 22. (a) Signal proposed by wavelet only. (b) Signal proposed by STL only.

TABLE IV
COMPARISON OF TRADITIONAL ALGORITHM AND PROPOSED ALGORITHM

Algorithm category	DIR	DSR
wavelet	0.68	1.08
STL decompose	0.87	0.73
Proposed algorithm	1.60	2.05

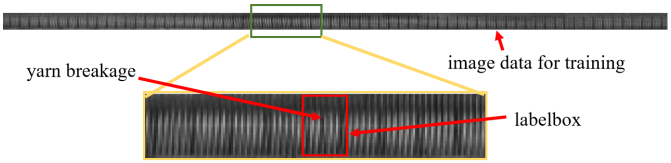

Fig. 23. (a) Image data for training and label box of yarn breakage.

In the process of data collection, we randomly select ten different positions within the field of view of one camera, and manually break the yarn. We collected 300 images at each location, and select the yarn breakage visible to the human eyes to label; finally, we obtained 880 defect image. Then, we cut out the yarn area of each picture for training, and the final image resolution is 1280∗32, because the yarn periodic texture is very similar to broken yarn characteristics. In the process of labeling, we control the width of the labeling box equal to yarn texture period, as shown in Fig. 23. Some key training parameters in the specific training process are shown in Table V, and the training result is shown in Table VI. After training, the trained model is used to detect two sets of data, the first data have 300 images all of which have defect, the second data are 500 normal images, and the result is shown in Fig. 24. And the data processed by the algorithm proposed in this article are shown in Fig. 25, where the gray value less than 200 is considered as defects, and the final result is shown in Fig. 26, where Fig. 26(a) shows data with defect and Fig. 26(b) shows data with no defect. By comparing Figs. 24 and 26, it can be seen that though the method based on deep learning can identify defects, the false negative cannot be avoided; although the false negative rate is not high, it will cause frequent alarms and cannot be used in industrial scene. In contrast, the proposed algorithm is more stable.

TABLE V
TRAINING PARAMETERS

Parameter	Value
Batch size	64
Number of epochs	436
Image resolution	1280*32
Number of training/testing image	880/800
Learning rate	0.001
Channels	1

TABLE VI
TRAINING RESULT

Parameter	Value
Loss	0.0946
mAP	96%

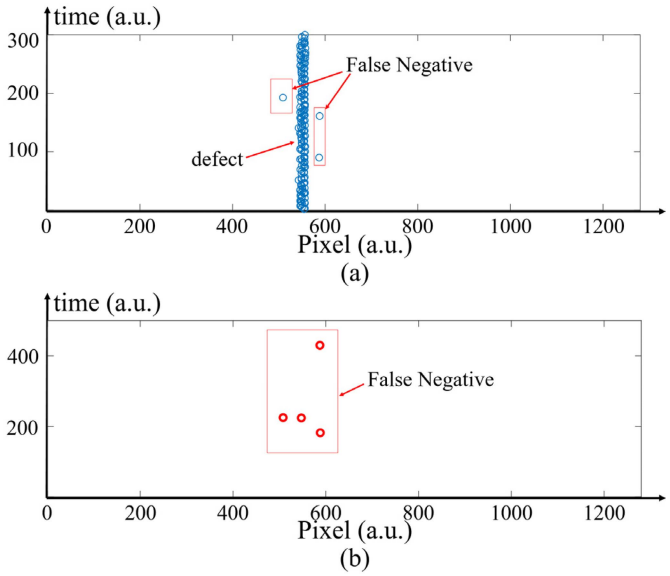

Fig. 24. (a) Detecting result of yolov4 for data with defect. (b) Detecting result of yolov4 for data with no defect.

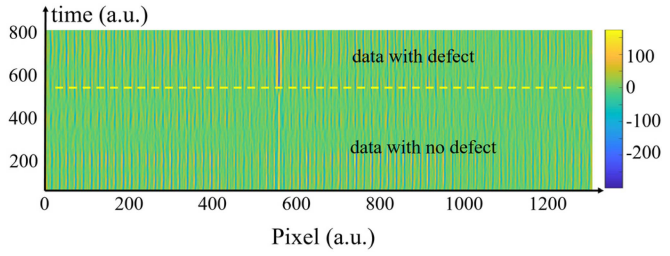

Fig. 25. Data processed by the algorithm proposed in this article.

In order to analyze the reasons for the false negative of deep learning, two of the images of false negative are shown in Fig. 27, where we can see characteristics similar to defects;

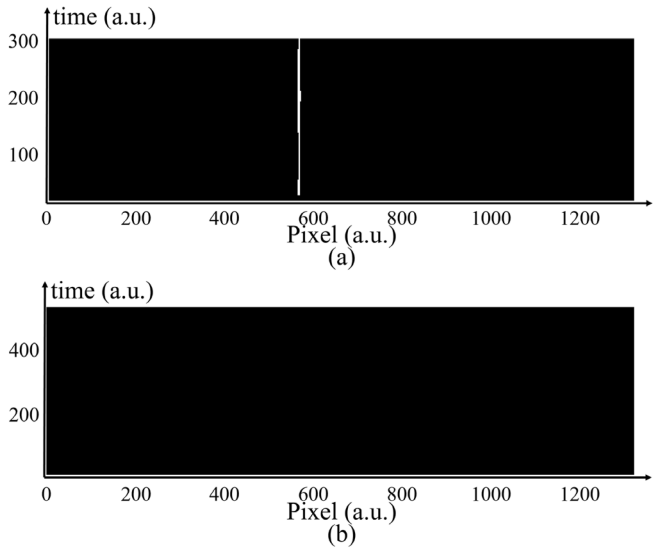

Fig. 26. (a) Detecting result of the proposed method for data with defect. (b) Detecting result of the proposed method for data with no defect.

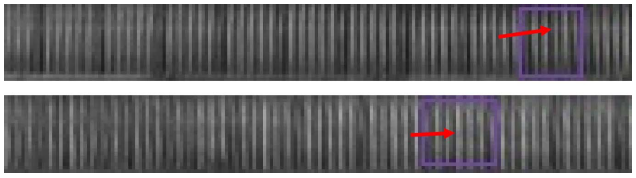

Fig. 27. Images of false negative.

TABLE VII
PROCESSING PARAMETERS OF THE WARP KNITTING MACHINE

Guide bar number	Diameter of yarns	Threading process
No. 1	200 μm	1 in, 1 out
No. 2	200 μm	1 in, 1 out
No. 3	30 μm	Fully threaded
No. 4	75 μm	Fully threaded
No. 5	75 μm	Fully threaded

it is not easy to distinguish even for the human eyes, which explains that the decline of the stability of deep learning is caused by the random noise similar to defect; however, because the proposed method in this article introduces the time domain signal processing method, even if there is noise at a certain moment, it will be filtered out by STL smoothing; therefore, it has better ability of anti-noise. However, in essence, method based on deep learning is still a kind of space domain method; if we combine this method with time domain method, the stability will be further improved, which can be used as a direction of future research.

D. Stability Experiments

In order to verify the stability of this method, the detection system is turned on for 120 h for the stability experiment, and the manual yarn breaking experiment is conducted. The machine processes are shown in Table VII. It can be calculated

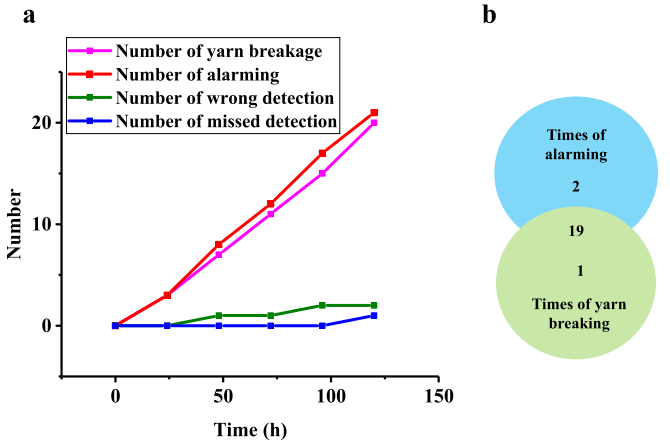

Fig. 28. 120-h continuous experiment is conducted to verify the stability of the method. The number of alarms, the number of yarn breakages, the wrong detections, and the missed detections are recorded in (a), and the summary of the results is shown in (b).

TABLE VIII
QUANTITATIVE ASSESSMENT OF THE EXPERIMENT

Evaluation index	Value
False Positive Rate	1.39e-9%
False Negative Rate	5%

that the machine has approximately 13 900 yarns in total, and five images are taken per second. It can be calculated that images of six billion yarns are taken per day. The final experimental results are shown in Fig. 28. Fig. 28(a) shows the detection result over time, where the red line is the number of alarms, and the blue line is the number of yarn breaks. Because of incorrect detections (gray line) and missed detections (yellow line), the number of alarms and the number of yarn breakages do not coincide. Fig. 28(b) shows the statistical results of Fig. 28(a), where the blue area is the number of alarms, the green area is the actual number of yarn breakages, and the intersection of the two is the number of positive checks. As the results show, during the 120-h experiment, the system had only two incorrect detections; and in the 20 yarn breaking experiments, 19 yarn breakages were detected, and the detection rate was up to 95%. The quantitative assessment of the experiment is shown in Table VIII. The table shows that the system can meet very demanding false negative rate requirements and FPR requirements at the same time. The detection error is caused because of the unstable factors in the weaving process, such as the abnormal vibration of the machine and changes in light environment, which can be further improved by stabilizing the factory lighting environment and regular maintenance of machine tools. The results prove that this method can achieve the long-term and stable detection of yarn breakage.

IV. CONCLUSION

This article proposes an optical reflection-based online yarn breakage detection method. Yarn breakages can be detected

by directly shooting the weaving area, and the feasibility of the method has been proven through several experiments.

1) A stable and reliable detection method is proposed, macrocapturing is applied to solve the problem that yarns are thin and dense, and a detection method based on the law of reflection is proposed to improve the SNR. Moreover, image processing based on wavelet and STL decomposition is proposed to achieve the accurate extraction of defects.
2) A detection system that can detect different layers of yarns is constructed. The detection rate of the method is proven to be as high as 95% after a 120-h continuous experiment, and the FPR is controlled at 1.39e−9%. The method is also proven to be suitable for different textile processes.
3) The proposed method is a successful application of the reflection method to the high-precision detection of non-Lambert objects, which has great enlightening significance for the high-precision anomaly detection of precision equipment. Here, we list two types of problems as an extension of this article. The first type is defect detection of flat parts such as ceramic tile, glass plate, and plastic board; first, reflection method is a high-precision way to highlight the defect in this kind of structures; second, during the transportation of these structures with the conveyor belt, the defects characteristics can also be characterized by anomalies of periodic signals. Another type is abnormal detection of rotary structure such as abnormal of blade rotation and radial runout detection of shaft, because the working processes of these structures are strictly periodic; through the change law of the reflected light, it is very suitable for troubleshooting through abnormal analysis of periodic signal; at the same time, because the reflected signal is very sensitive to the angle, this method can also achieve high precision.

ACKNOWLEDGMENT

The authors are grateful to engineers from Hua Yu Zheng Ying Group Company and Natong Company for their help in preparing the experiments.

REFERENCES

[1] M. R. Driels and U. S. Pathre, "Vision-based automatic theodolite for robot calibration," *IEEE Trans. Robot. Autom.*, vol. 7, no. 3, pp. 351–360, Jun. 1991.
[2] F. Zheng and B. Kong, "Calibration of linear structured light system by planar checkerboard," in *Proc. Int. Conf. Inf. Acquisition*, Jun. 2004, pp. 344–346.
[3] S. Zhang, "Recent progresses on real-time 3D shape measurement using digital fringe projection techniques," *Opt. Lasers Eng.*, vol. 48, no. 2, pp. 149–158, Feb. 2010.
[4] J. Balzer and S. Werling, "Principles of shape from specular reflection," *Measurement*, vol. 43, no. 10, pp. 1305–1317, Dec. 2010.
[5] C. Faber, E. Olesch, R. Krobot, and G. Häusler, "Deflectometry challenges interferometry: The competition gets tougher," *Proc. SPIE*, vol. 8493, Sep. 2012, Art. no. 84930R.
[6] R. Lal, "A new, optical-lever based atomic force microscope," *J. Appl. Phys*, vol. 76, no. 2, pp. 796–799, 1994.
[7] F. Y. Khalili, "The 'optical lever' intracavity readout scheme for gravitational-wave antennae," *Phys. Lett. A*, vol. 298, nos. 5–6, pp. 308–314, 2002.
[8] J. Bhang, Y. Roh, and D. Jeong, "A reflectometry approach for rippling defect measurement on high glossy surface," in *Proc. Int. Symp. Optomechatronic Technol.*, Nov. 2014, pp. 47–49.
[9] Q. Luo, X. Fang, L. Liu, C. Yang, and Y. Sun, "Automated visual defect detection for flat steel surface: A survey," *IEEE Trans. Instrum. Meas.*, vol. 69, no. 3, pp. 626–644, Mar. 2020.
[10] F.-C. Chen and M. R. Jahanshahi, "NB-FCN: Real-time accurate crack detection in inspection videos using deep fully convolutional network and parametric data fusion," *IEEE Trans. Instrum. Meas.*, vol. 69, no. 8, pp. 5325–5334, Aug. 2020.
[11] M. Stoppa and A. Chiolerio, "Wearable electronics and smart textiles: A critical review," *Sensors*, vol. 14, no. 7, pp. 11957–11992, Jul. 2014.
[12] T. Agcayazi, M. McKnight, H. Kausche, T. Ghosh, and A. Bozkurt, "A finger touch force detection method for textile based capacitive tactile sensor arrays," in *Proc. IEEE Sensors*, Oct. 2016, pp. 1–3.
[13] B. Zhou *et al.*, "Textile pressure mapping sensor for emotional touch detection in human-robot interaction," *Sensors*, vol. 17, no. 11, p. 2585, Nov. 2017.
[14] V. Carvalho, J. G. Pinto, J. L. Monteiro, R. M. Vasconcelos, and F. O. Soares, "Yarn parameterization based on mass analysis," *Sens. Actuators A, Phys.*, vol. 115, nos. 2–3, pp. 540–548, Sep. 2004.
[15] G. F. Chen, H. C. Sun, L. L. Zhai, and L. L. Peng, "A capacitance based circuit design for yarn breaking detection," in *Advanced Materials Research*, vol. 562. Beijing, China: NCNST, 2012, pp. 1840–1843.
[16] L. D. Jun, "The research of broken filaments detection device on viscose filament yarn," in *Proc. Int. Conf. Comput. Intell. Secur. Workshops (CISW)*, Dec. 2007, pp. 910–913.
[17] W. Lu, X. Lu, C. Zhu, Q. Liu, and H. Zhang, "Solving three key problems of the SAW yarn tension sensor," *IEEE Trans. Electron Devices*, vol. 59, no. 10, pp. 2853–2855, Oct. 2012.
[18] E. Musa, "Line laser-based break sensor that detects light spots on yarns," *Opt. Lasers Eng.*, vol. 47, nos. 7–8, pp. 741–746, Jul. 2009.
[19] E. Musa, "Line-laser-based yarn shadow sensing break sensor," *Opt. Lasers Eng.*, vol. 49, no. 3, pp. 313–317, Mar. 2011.
[20] H. Y. T. Ngan, G. K. H. Pang, and N. H. C. Yung, "Automated fabric defect detection-A review," *Image Vis. Comput.*, vol. 29, no. 7, pp. 442–458, Jun. 2011.
[21] C.-H. Chan and G. K. H. Pang, "Fabric defect detection by Fourier analysis," *IEEE Trans. Ind. Appl.*, vol. 36, no. 5, pp. 1267–1276, Sep. 2000.
[22] S. Mei, H. Yang, and Z. Yin, "An unsupervised-learning-based approach for automated defect inspection on textured surfaces," *IEEE Trans. Instrum. Meas.*, vol. 67, no. 6, pp. 1266–1277, Jun. 2018.
[23] D. Schneider and T. Aach, "Vision-based in-line fabric defect detection using yarn-specific shape features," *Proc. SPIE*, vol. 8300, Feb. 2012, Art. no. 83000G.
[24] S. Mei, Y. Wang, and G. Wen, "Automatic fabric defect detection with a multi-scale convolutional denoising autoencoder network model," *Sensors*, vol. 18, no. 4, p. 1064, Apr. 2018.
[25] M. R. Minar and J. Naher, "Recent advances in deep learning: An overview," 2018, *arXiv:1807.08169*. [Online]. Available: http://arxiv.org/abs/1807.08169
[26] G. Hu, J. Huang, Q. Wang, J. Li, Z. Xu, and X. Huang, "Unsupervised fabric defect detection based on a deep convolutional generative adversarial network," *Textile Res. J.*, vol. 90, nos. 3–4, pp. 247–270, Feb. 2020.
[27] P. M. Bhatt *et al.*, "Image-based surface defect detection using deep learning: A review," *J. Comput. Inf. Sci. Eng.*, vol. 21, no. 4, pp. 1–23, Aug. 2021.
[28] B. Wei, K. Hao, X.-S. Tang, and Y. Ding, "A new method using the convolutional neural network with compressive sensing for fabric defect classification based on small sample sizes," *Textile Res. J.*, vol. 89, no. 17, pp. 3539–3555, Sep. 2019.
[29] P. R. Jeyaraj and E. R. S. Nadar, "Effective textile quality processing and an accurate inspection system using the advanced deep learning technique," *Textile Res. J.*, vol. 90, nos. 9–10, pp. 971–980, May 2020.
[30] Z. Zhao, K. Gui, and P. Wang, "Fabric defect detection based on cascade faster R-CNN," in *Proc. 4th Int. Conf. Comput. Sci. Appl. Eng.*, Oct. 2020, pp. 1–6.
[31] J. Jing, D. Zhuo, H. Zhang, Y. Liang, and M. Zheng, "Fabric defect detection using the improved YOLOv3 model," *J. Eng. Fibers Fabrics*, vol. 15, Jan. 2020, Art. no. 155892502090826.
[32] Z. Liu, J. Cui, C. Li, M. Wei, and Y. Yang, "Fabric defect detection based on lightweight neural network," in *Proc. Chin. Conf. Pattern Recognit. Comput. Vis. (PRCV)*, Cham, Switzerland: Springer, Nov. 2019, pp. 528–539.

[33] J. Jing, Z. Wang, M. Rätsch, and H. Zhang, "Mobile-UNet: An efficient convolutional neural network for fabric defect detection," *Textile Res. J.*, May 2020, Art. no. 004051752092860. [Online]. Available: https://journals.sagepub.com/doi/abs/10.1177/0040517520928604
[34] N. O'Mahony *et al.*, "Deep learning vs. Traditional computer vision," in *Proc. Sci. Inf. Conf.*, 2019, pp. 128–144.
[35] X. Xie, "A review of recent advances in surface defect detection using texture analysis techniques," in *ELCVIA, Electronic Letters on Computer Vision and Image Analysis*. Madrid, Spain: Centre de Visio per Computador, 2008, pp. 1–22.
[36] M. Swain and D. Ballard, "Indexing via color histograms," *Int. J. Comput. Vis.*, vol. 7, no. 1, pp. 11–32, 1990.
[37] R. M. Haralick, K. Shanmugam, and I. Dinstein, "Textural features for image classification," *IEEE Trans. Syst., Man, Cybern.*, vol. SMC-3, no. 6, pp. 610–621, Nov. 1973.
[38] E. J. Wood, "Applying Fourier and associated transforms to pattern characterization in textiles," *Textile Res. J.*, vol. 60, no. 4, pp. 212–220, Apr. 1990.
[39] T. Ojala, M. Pietikäinen, and T. Mäenpää, "Multiresolution gray-scale and rotation invariant texture classification with local binary patterns," *IEEE Trans. Pattern Anal. Mach. Intell.*, vol. 24, no. 7, pp. 971–987, Jul. 2002.
[40] F. M. Vilnrotter, R. Nevatia, and K. E. Price, "Structural analysis of natural textures," *IEEE Trans. Pattern Anal. Mach. Intell.*, vol. PAMI-8, no. 1, pp. 76–89, Jan. 1986.
[41] B. B. Mandelbrot, *The Fractal Geometry of Nature*. New York, NY, USA: W.H. Freeman, 1983.
[42] G.-H. Hu, G.-H. Zhang, and Q.-H. Wang, "Automated defect detection in textured materials using wavelet-domain hidden Markov models," *Opt. Eng.*, vol. 53, no. 9, Sep. 2014, Art. no. 093107.
[43] N. A. Bakar, S. Rosbi, and K. Uzaki, "Forecasting cryptocurrency price movement using moving average method: A case study of bitcoin cash," *Int. J. Adv. Res.*, vol. 7, no. 12, pp. 609–614, Dec. 2019.
[44] E. B. Dagum and S. Bianconcini, *Seasonal Adjustment Methods and Real Time Trend-Cycle Estimation*. New York, NY, USA: Springer, 2016.
[45] R. B. Cleveland, W. S. Cleveland, J. E. McRae, and I. Terpenning, "STL: A seasonal-trend decomposition," *J. Off. Statist.*, vol. 6, no. 1, pp. 3–73, 1990.
[46] A. Bochkovskiy, C.-Y. Wang, and H.-Y. Mark Liao, "YOLOv4: Optimal speed and accuracy of object detection," 2020, *arXiv:2004.10934*. [Online]. Available: http://arxiv.org/abs/2004.10934
[47] Z. Yu, Y. Shen, and C. Shen, "A real-time detection approach for bridge cracks based on YOLOv4-FPM," *Autom. Construct.*, vol. 122, Feb. 2021, Art. no. 103514.

Ning Yan was born in Shanxi, China, in 1994. He received the B.S. degree in measurement and control technology and instrument from Tianjin University, Tianjin, China, in 2017, where he is currently pursuing the Ph.D. degree in instrument science.

His research interests include computer vision and precise measurement.

Linlin Zhu was born in Shandong, China, in 1989. He received the Ph.D. degree in instrument science and technology from Tianjin University, Tianjin, China, in 2021.

He is engaged in precise 3-D measurement.

Hongmai Yang was born in Fujian, China, in 1996. He received the B.S. degree in measurement and control technology and instrument from Tianjin University, Tianjin, China, in 2018, where he is currently pursuing the M.S. degree in instrument and meter engineering.

His research interests include computer vision and precise measurement.

Nana Li, photograph and biography not available at the time of publication.

Xiaodong Zhang received the Ph.D. degree in measurement science and technology from Tianjin University, Tianjin, China, in 2007.

He is currently a Professor with the School of Precision Instrument and Optical Electronic Engineering, Tianjin University. He has been the Head of "Ultra-precision machining and freeform optics manufacture" group at Centre of MicroNano Manufacturing Technology (MNMT) since 2008. His research interests include ultraprecision machining, optical metrology, and applications of complex surfaces.